Accepted Manuscript

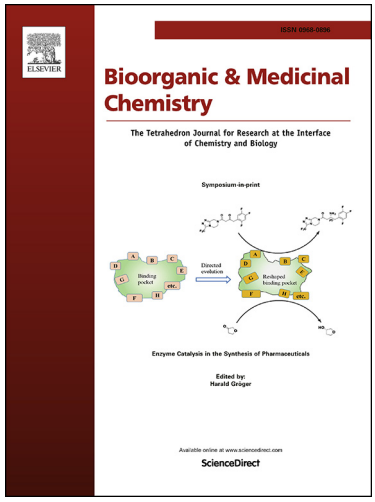

Small Molecule Inhibition of MicroRNA-21 Expression Reduces Cell Viability and Microtumor Formation

Nicholas Ankenbruck, Rohan Kumbhare, Yuta Naro, Meryl Thomas, Laura Gardner, Cole Emanuelson, Alexander Deiters

PII: S0968-0896(19)30047-1
DOI: https://doi.org/10.1016/j.bmc.2019.05.044
Reference: BMC 14931

To appear in: *Bioorganic & Medicinal Chemistry*

Received Date: 1 February 2019
Revised Date: 1 May 2019
Accepted Date: 28 May 2019

Please cite this article as: Ankenbruck, N., Kumbhare, R., Naro, Y., Thomas, M., Gardner, L., Emanuelson, C., Deiters, A., Small Molecule Inhibition of MicroRNA-21 Expression Reduces Cell Viability and Microtumor Formation, *Bioorganic & Medicinal Chemistry* (2019), doi: https://doi.org/10.1016/j.bmc.2019.05.044

This is a PDF file of an unedited manuscript that has been accepted for publication. As a service to our customers we are providing this early version of the manuscript. The manuscript will undergo copyediting, typesetting, and review of the resulting proof before it is published in its final form. Please note that during the production process errors may be discovered which could affect the content, and all legal disclaimers that apply to the journal pertain.

ACCEPTED MANUSCRIPT

Small Molecule Inhibition of MicroRNA-21 Expression Reduces Cell Viability and Microtumor Formation

Nicholas Ankenbruck‡, Rohan Kumbhare‡, Yuta Naro‡, Meryl Thomas, Laura Gardner, Cole Emanuelson, and Alexander Deiters*

‡ The authors contributed equally.

Department of Chemistry, University of Pittsburgh, Pittsburgh, Pennsylvania 15260, United States, deiters@pitt.edu

ABSTRACT

MicroRNAs (miRNAs) are short, non-coding RNA molecules estimated to regulate expression of a large number of protein-coding genes and are implicated in a variety of biological processes such as development, differentiation, proliferation, and cell survival. Dysregulation of miRNAs has been attributed to the onset and progression of various human diseases, including cancer. MicroRNA-21 (miR-21), one of the most established oncogenic miRNAs, is found to be upregulated in a wide range of cancers making it an attractive therapeutic target. Employment of a luciferase-based live-cell reporter assay in a high-throughput screen of >300,000 small molecules led to the discovery of a new class of ether-amide miR-21 inhibitors. Following a structure-activity relationship study, an optimized lead molecule was found to inhibit miR-21 transcription. Furthermore, the inhibitor demonstrated cytotoxicity in a cervical cancer cell line via induction of apoptosis and was capable of reducing microtumor formation in a long-term clonogenic assay. Altogether, this work reports the discovery of a new small molecule inhibitor of miR-21 and demonstrates its potential as an alternative approach in cancer therapy.

1. INTRODUCTION

ACCEPTED MANUSCRIPT

MicroRNAs (miRNAs) are small, non-coding RNA molecules of 20-22 nucleotides in length that regulate gene expression. In the canonical pathway, miRNAs repress translation by hybridizing to a complementary sequence in the 3' untranslated region (3' UTR) of target mRNAs.[1] In addition to inhibition of translation initiation factor binding and recruitment of deadenylases, miRNAs have been shown to inhibit ribosome-mediated elongation and to displace translation initiation factors post-translation initiation, ultimately resulting in mRNA decay. Recently, miRNAs have also been predicted to repress translation via binding to the 5' UTR, coding domain sequences, and open reading frames.[2] While some experimental studies have provided support to these hypotheses,[3-5] the generality and extent to which these alternative mechanisms contribute to miRNA-mediated translational repression remains unclear. MiRNA biogenesis occurs via a dedicated maturation pathway,[6] beginning with transcription of primary miRNAs (pri-miRNAs) by RNA polymerase II or III. Pri-miRNAs are subsequently cleaved by Drosha, producing a short hairpin known as precursor-miRNA (pre-miRNA)[7] which is then exported from the nucleus to the cytoplasm[8] where it is further processed by Dicer to yield the mature miRNA duplex. The guide strand of mature miRNA is subsequently loaded into the RNA-Induced Silencing Complex (RISC), which then modulates gene expression via sequence-specific binding to the target mRNA.[9,10] Using photoactivatable ribonucleoside enhanced cross-linking and immunoprecipitation (PAR-CLIP), it was shown that miRNAs regulate 21% of protein-coding genes in humans.[11] Given the numerous genes targeted by miRNAs, it's not surprising that their dysregulation contributes to the development of various human diseases,[12-14] most notably cancer.[15-18]

MicroRNA-21 (miR-21) is an oncogenic miRNA found to be upregulated in almost all cancers and it plays a critical role in carcinogenesis via repression of several important tumor suppressors.[19] Furthermore, miR-21 has been implicated in modulating drug resistance via inhibition of programmed cell death protein 4 (PDCD4), an important target of miR-21, and a

ACCEPTED MANUSCRIPT

subsequent increase in cellular inhibitor of apoptosis protein 2 (c-IAP2) activity.[20] Additionally, miR-21-mediated silencing of phosphatase and tensin homolog (PTEN) can lead to chemoresistance via activation of the Akt and ERK pathways in cancer cells.[21] Due to its implications in cancer, miR-21 has emerged as a potential target for therapeutic approaches, including small molecules.[22-28]

Here, we report a new class of small molecules that selectively inhibit miR-21 and that were discovered through a high-throughput screen using a previously developed cell-based reporter assay.[23] Through extensive structure-activity relationship (SAR) studies, we identified an analog with improved activity compared to the initial hit compounds. Mode of action studies suggest that the small molecule inhibits miR-21 at the transcriptional step of miRNA biogenesis. Furthermore, pre-therapeutic evaluation of the compound showed that small molecule-mediated inhibition of miR-21 led to a decrease in cervical cancer cell proliferation and microtumor formation, as well as induction of apoptosis via capase-3/7 activation.

2. RESULTS AND DISCUSSION

Previously, we developed a luciferase-based live cell reporter assay for the discovery of small molecule modulators of miR-21 function.[23] Briefly, a binding site complementary to miR-21 was inserted downstream of a firefly luciferase gene in the 3' UTR, such that expression of the reporter in the presence of endogenous miR-21 would lead to a reduction in luminescence (**Fig. 1A**). Inhibition of miR-21 function relieves translational repression of firefly luciferase and leads to an increase in luminescence signal. The reporter construct was stably introduced into HeLa cells via lentiviral transduction to afford a cell line amenable to the high-throughput screening of 333,519 compounds (PubChem AID 2289), which was carried out by the National Cancer

ACCEPTED MANUSCRIPT

Institute. Filtering hits through secondary assays using a miR-30a reporter (PubChem AID 2507) and an *in vitro* firefly luciferase assay (PubChem AID 493175) yielded 58 potential inhibitors that were not general inhibitors of the miRNA pathway and were not false positives due to non-miRNA specific firefly luciferase activation.[29] Compound **1** (PubChem CID 71233585; **Fig. 1B**) was selected for further investigation based on its promising activity and synthetic accessibility.

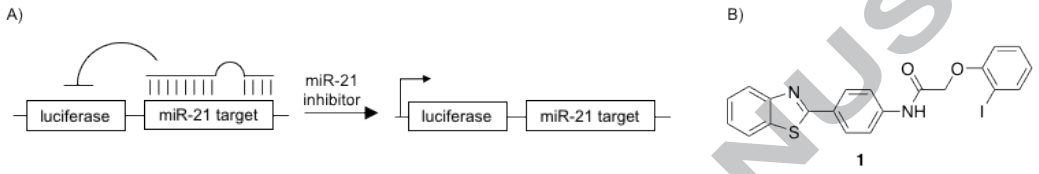

Figure 1. A) Design of a luciferase-based live-cell reporter for high-throughput screening of small molecule modulators of miR-21 function. miR-21 binds to a complementary sequence in the 3' UTR of the luciferase gene inhibiting translation and resulting in a decrease in luciferase expression. Presence of a small molecule inhibitor of miR-21 transcription relieves translational repression of the reporter, resulting in an increase in luciferase levels. B) Chemical structure of hit compound **1** identified in the high-throughput screen.

Analogs of the initial hit **1** were synthesized using a synthetic route that allowed for facile functionalization of numerous positions across the structure (**Scheme S1**). Commercially available *ortho*-substituted anilines **2** were readily reacted with **3** via a condensation reaction in polyphosphoric acid to obtain the resulting benzoimidazoles, benzothiazoles, and benzoxazoles **4**. Subsequent reaction with acetyl chloride provided the linker region in **5** which readily underwent nucleophilic substitution with phenols, thiols and anilines in the presence of cesium carbonate to yield the final products.

Using this synthetic route, a small panel of analogs was generated and their biological activity was evaluated using the HeLa-miR21-Luc cell line (**Fig. 2**). The initial hit **1** demonstrated

ACCEPTED MANUSCRIPT

modest activity, inducing a 1.55-fold increase in luciferase signal following treatment at 10 μM for 48 h. Removal of the iodide to yield **6** resulted in only a very minor improvement in activity, while loss of the iodide along with introduction of a *para*-methoxy group in **7** had little to no effect on activity. Turning towards modifying the benzothiazole ring, the benzoxazole derivative of **1** yielded **8**, which maintained the same activity as the parent compound. Keeping the benzoxazole and removal of the iodide resulted in **9**, which showed no change in activity, while introduction of a *para*-methoxy to yield **10** abolished all activity. Expanding upon **9**, addition of a 5-chloro modification to the benzoxazole led to in **11**, which demonstrated an 85% enhancement in activity compared to the initial hit **1**. Furthermore, addition of a *para*-methoxy substitution to **11** to yield **12** further enhanced activity, eliciting a 314% improvement compared to **1**. Continuing from the promising results obtained from **11** and **12**, analogs containing benzimidazoles (**13** and **14**) were synthesized, however, only a loss in activity was observed in both cases.

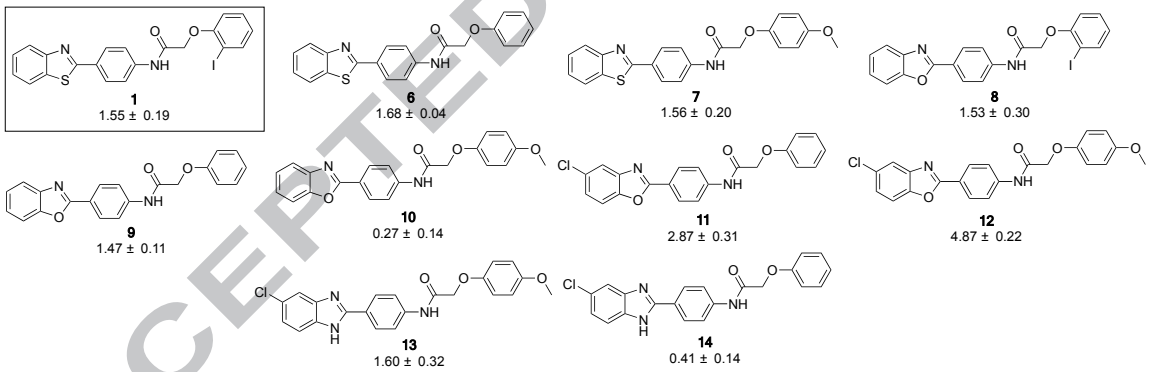

Figure 2. Activity of compounds **1** and **6** – **14** in the HeLa-miR21-Luc assay. Values represent fold-changes in luminescence signal in the HeLa-miR21-Luc stable cell line normalized to cell viability and relative to a DMSO control. Data represents the average ± standard deviation from at least three independent experiments.

To build upon the improvement in activity seen in **11** and **12**, an additional round of analogs was generated containing further modification to each respective compound. For **11**, moving the 5-

ACCEPTED MANUSCRIPT

chloride to the 6-position yielded **16**, which had only a minor impact on activity. Changing the ether-amide linker from the *para*- to the *meta*-position yielded analogs **17** and **18**, which resulted in a loss of activity. The importance of the ether-amide linker was investigated by synthesizing **19** bearing a shorter carbamate linker (**Scheme S2**). Compound **19** elicited a 35% increase in activity relative to **11** and a 249% increase relative to the initial hit **1**. Analogous modifications were also made to **12** to produce **20**, **21**, **22**, and **23**, however, only reduced activity was observed in this set of analogs (**Fig. 3**).

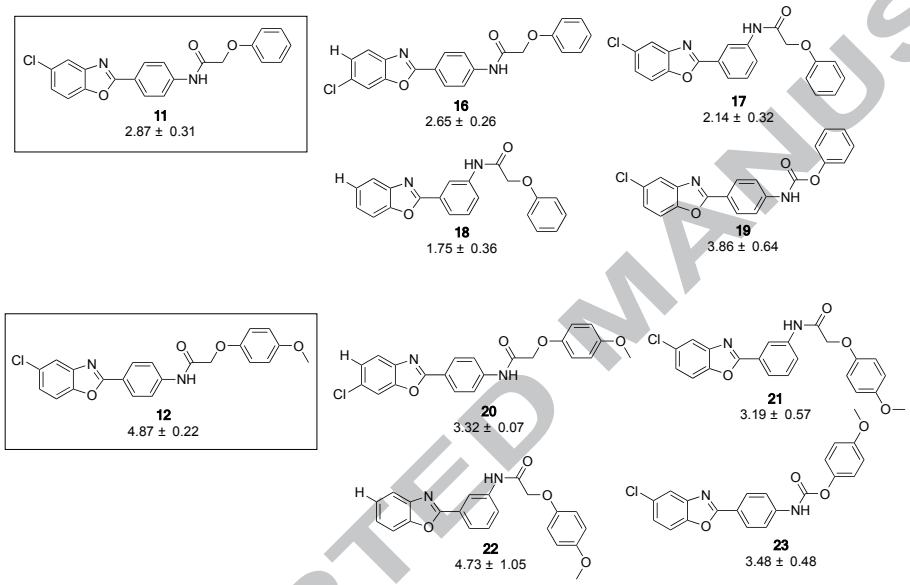

Figure 3. Activity of compounds **16** – **23** in the HeLa-miR21-Luc assay. Values represent fold-changes in luminescence signal in the HeLa-miR21-Luc stable cell line normalized to cell viability and relative to a DMSO control. Data represents the average ± standard deviation from at least three independent experiments.

With **12** remaining the most potent inhibitor identified thus far, we decided to investigate further modifications to its structure. To this end, analogs containing modifications to the ether-amide linker and the central aniline ring were synthesized and their activity was tested in the HeLa-miR21-Luc stable cell line (**Fig. 4**). Replacement of the ether-amide linker with a thioether amide

ACCEPTED MANUSCRIPT

linker produced analog **24** which exhibited a 54% decrease in activity relative to **12**. Furthermore, incorporation of an amino-amide linker in place of the ether-amide linker resulted in **25** and completely abolished activity. Replacement of the central aniline ring with a naphthalene (**26**) or benzothiazole (**27**) was also detrimental to activity. Lastly, alkylation of the amide nitrogen in **12** with a methyl or propargyl group, **28** and **29** respectively (**Scheme S3**), abolished activity compared to the parent compound **12**. Taken together, these results confirmed the importance of the ether-amide linker to activity and thus we decided to maintain this moiety moving forward with additional analogs.

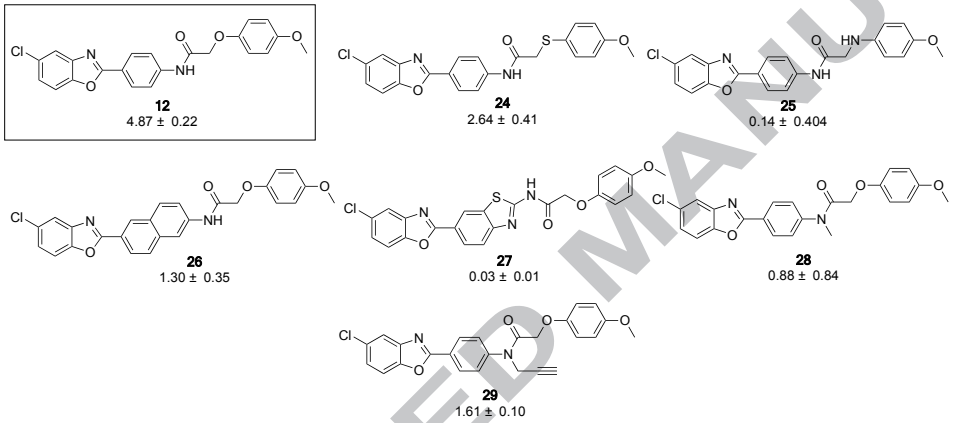

Figure 4. Activity of compounds **24** – **29** in the HeLa-miR21-Luc assay. Values represent fold-changes in luminescence signal in the HeLa-miR21-Luc stable cell line normalized to cell viability and relative to a DMSO control. Data represents the average ± standard deviation from at least three independent experiments.

Building upon the generated structure-activity information, we decided to synthesize an additional set of analogs based on **12**, but containing more diverse changes to the two distal ring systems while maintaining the structure of the central region of the scaffold. To this end, additional analogs were synthesized and tested in the miR-21 luciferase reporter (**Fig. 5)**. Moving the *para*-methoxy to the *meta*-position resulted in **30**, which displayed similar activity to **12**. Replacement of the *para*-methoxy with a nitrile (**31**), fluorine (**32**), nitro (**33**), or phenyl (**34**)

ACCEPTED MANUSCRIPT

group all resulted in losses of activity. Similarly, introduction of a *para*-isopropyl in conjunction with a *meta*-methyl group (**35**) led to a 46% decrease in activity. Interestingly, replacement of the 5-chloro with a 5-fluoro in conjunction with (**36**) or without (**37**) the *para*-methoxy group also reduced activity, providing evidence that the 5-position may be highly sensitive to modifications. To further support this, introduction of a bromine at the 5-position (**38**) resulted in a 27% increase in activity compared to the parent compound **12.** Surprisingly, introduction of a phenyl group at the 5-position (**39**) had an even greater impact on activity, demonstrating a 62% improvement in activity compared to **12**, and a 508% increase in activity relative to the initial hit **1**. Conversion of the benzoxazole to a pyridinyloxazole (**40**) led to a loss in activity compared to **1** and further supports the critical nature of the 5-position on the benzoxazole.

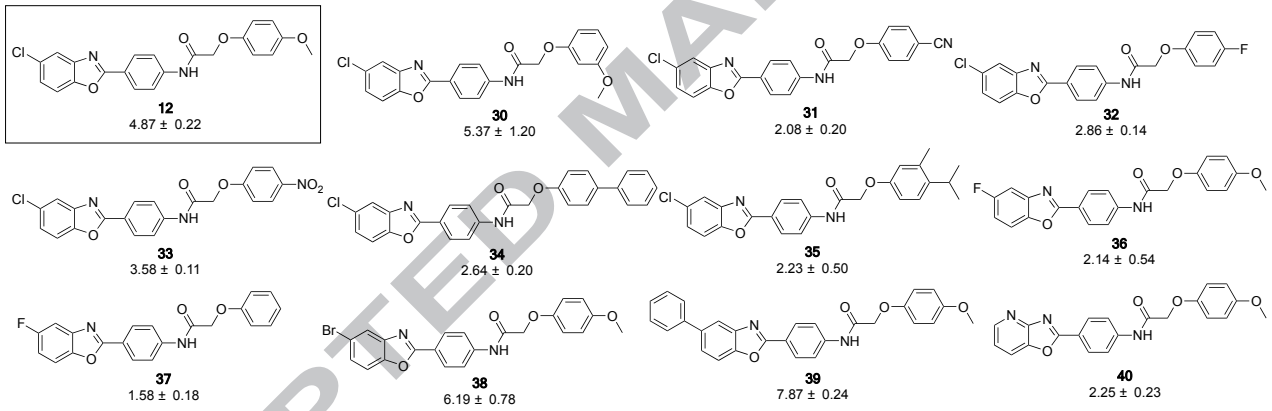

Figure 5. Activity of compounds **30** – **40** in the HeLa-miR21-Luc assay. Values represent fold-changes in luminescence signal in the HeLa-miR21-Luc stable cell line normalized to cell viability and relative to a DMSO control. Data represents the average ± standard deviation from at least three independent experiments.

Overall, the SAR studies suggest several key positions on the inhibitor that appear sensitive to modification, including the ether-amide linker core and the 5-position on the benzoxazole ring system. With the promising and improved candidates **12**, **30**, **38**, and **39** in hand, we next evaluated their biological activity and confirmed their function as miR-21 inhibitors.

ACCEPTED MANUSCRIPT

2.2. Secondary assays to confirm activity of miR-21 inhibitors

Firstly, the HeLa-miR21-Luc reporter cell line was treated in dose-response with the most promising analogs, and **12**, **30**, **38**, and **39** all demonstrated reporter activation in a dose-dependent fashion with EC_{50} values of 6.7 μM, 4.7 μM, 6.4 μM, and 3.5 μM, respectively (**Fig. 6**).

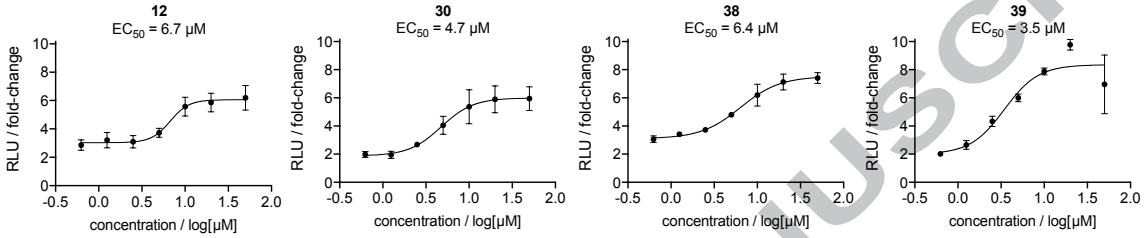

Figure 6. Treatment of HeLa-miR21-Luc stable reporter cells with varying concentrations of inhibitor **12**, **30**, **38**, or **39** followed by a Bright-Glo assay. Luciferase signal was first normalized to cell viability and then to a DMSO control. Errors bars represent standard deviations from three independent experiments. EC_{50} values were determined by fitting data to a nonlinear regression analysis in GraphPad Prism software.

Firefly luciferase inhibitors have been previously identified as false positive hits in high-throughput screens due to luciferase enzyme stabilization in cells.[30] Because this is a documented concern when using luciferase reporter assays,[29] we decided to evaluate the effect of **12**, **30**, **38**, and **39** on luciferase activity in a biochemical assay. Treatment with the positive control firefly luciferase inhibitor PTC-124[19] led to a 94% reduction in enzyme activity. While treatment with **12** elicited no significant reduction in luciferase activity, treatment with **30**, **38**, and **39** all led to 44, 38, and 27% reductions in luminescence signal, respectively (**Fig. 7A**). To further validate whether these inhibitors act on the miRNA pathway, we transfected HeLa cells with a psiCHECK-empty reporter (containing a sequence not targeted by any known miRNA) followed by treatment with the compounds at 10 μM for 48 h. The positive control PTC-124 and

ACCEPTED MANUSCRIPT

compounds **30**, **38**, and **39** induced an increase in luminescence signal ranging from 1.5 to 1.8-fold, while compound **12** only showed a minor increase in luciferase activity (**Fig. 7B**). These biochemical and cell-based results indicate that **30**, **38**, and **39** may have inflated activity profiles in the HeLa-miR21-Luc assay due to off-target binding to the firefly luciferase enzyme. Taking both the dose-response and *in vitro* firefly luciferase data into account, we decided to carry **12** forward as the primary candidate for further biological testing.

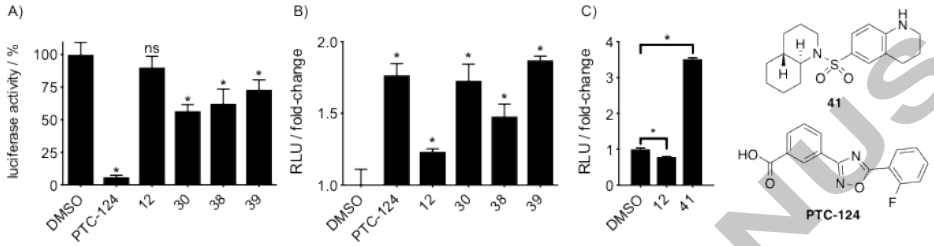

Figure 7. Evaluation of selectivity of lead compounds. A) Incubation of recombinant firefly luciferase with inhibitors **12**, **30**, **38**, or **39** at 10 μM, followed by a Bright-Glo assay. PTC-124, a known firefly luciferase inhibitor, was included as a positive control. B) Transfection of HeLa cells with the psiCHECK-empty plasmid followed by treatment with compounds **12**, **30**, **38**, and **39** or the positive control at 10 μM. A dual luciferase assay was performed after 48 h. RLU values represent firefly luciferase luminescence signal normalized to *Renilla* luciferase luminescence signal. C) Treatment of Huh7-miR122 stable cells with **12** (10 μM) or positive control **41** (10 μM). A dual luciferase assay was performed after 48 h. RLU values represent *Renilla* luciferase luminescence signal normalized to firefly luciferase luminescence signal. All data were normalized to DMSO treatment (negative control) and errors bars represent standard deviations from three independent experiments. Statistical significance was determined using an unpaired t-test, * $P < 0.05$, ns $P \geq 0.05$.

Next, we tested if **12** is a general miRNA pathway inhibitor or if it has selectivity for miR-21. To this end, we employed an additional stable reporter cell line, Huh7-miR122, which places *Renilla* luciferase expression under the control of miR-122 activity.[31] Treatment with **12** (10 μM) elicited only a minor 0.2-fold reduction in *Renilla* luciferase signal, demonstrating that **12** does not inhibit miR-122 activity (**Fig. 7C**). As a positive control, cells were also treated with **41**, a known miR-122 inhibitor,[31] which induced a >3.5-fold increase in luminescence, confirming functionality of the assay. Taken together, these results indicate that **12** shows some level of selectivity for miR-21 and is not a general miRNA pathway inhibitor.

ACCEPTED MANUSCRIPT

2.3. Identification of preliminary mode of action

To explore the mechanism by which **12** inhibits miR-21 function, levels of mature miR-21 were measured via reverse transcription quantitative PCR (RT-qPCR) after treatment with **12**. To ensure that the effects were not cell line dependent, three different cancer cell lines were tested. These cell lines included the parental line of the HeLa-miR21-Luc stable reporter cell line, HeLa cervical carcinoma cells, along with A549 non-small cell lung carcinoma cells, and SKOV3 ovarian cancer cells. Each cell line was treated with **12** (10 μM) or DMSO (0.1%) for 48 h, followed by miRNA isolation and quantification using RT-qPCR. In HeLa cells, a 57% reduction was observed (**Fig. 8A**), while in A549 and SKOV3 cells, 33% and 31% reductions were detected, respectively (**Fig. S1**). These results support a mechanism by which treatment with **12** results in depletion of mature miR-21 and subsequent reduction of miR-21 regulatory functions. To determine if **12** inhibits miR-21 maturation via binding directly to pre-miR-21, melting curve analyses were carried out in the presence of DMSO or **12**. The melting temperature of pre-miR-21 in the presence of DMSO control was measured to be 56.0 °C. The presence of **12** (10 μM) had no effect on melting temperature yielding a T_m of 56.2 °C (**Fig. S2**). These results indicate that **12** does not directly interact with miR-21 RNA and that miR-21 levels are likely impacted via an alternative mechanism.

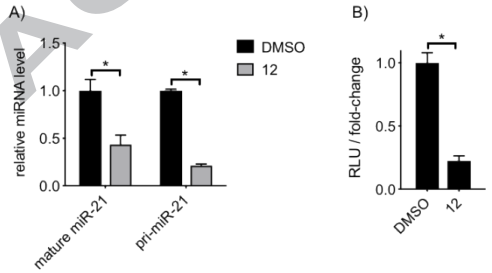

Figure 8. A) Treatment of HeLa cells with **12** (10 μM) for 48 h, followed by RT-qPCR analysis of mature miR-21 or primary miR-21 (pri-miR-21). B) Transfection of HeLa cells with a miR-21 promoter gene expression reporter followed by treatment with **12** (10 μM). A Bright-Glo assay was performed after 48 h.

ACCEPTED MANUSCRIPT

Data was normalized to DMSO treatment (negative control) and errors bars represent standard deviations from three independent experiments. Statistical significance was determined using an unpaired t-test, * $P < 0.05$.

To further investigate what step of the miR-21 biogenesis pathway our inhibitor may be targeting, primary miR-21 levels were analyzed via RT-qPCR in HeLa cells after treatment with **12** (10 μM) for 48 h. Interestingly, a marked 79% decrease in primary miR-21 levels was observed following treatment (**Fig. 8A**). This result supports a mechanism by which **12** is inhibiting transcription of the miR-21 gene, resulting in depletion of primary miR-21 levels. To confirm that compound **12** inhibits miR-21 transcription, HeLa cells were transfected with a previously described luciferase reporter construct that monitors miR-21 promoter activity, pGL4-miR21P,[22] and were treated with DMSO or **12** (10 μM) for 48 h. As expected, treatment with **12** resulted in a 78% decrease in miR-21 promoter activity compared to DMSO control (**Fig. 8B**). This result directly supports the drastic reduction in primary miR-21 levels observed via RT-qPCR and further suggests a mechanism of action by which **12** inhibits transcription of the miR-21 gene.

*2.4. Functional studies of **12***

Next, we evaluated whether **12**-mediated inhibition of miR-21 could elicit a therapeutic response in HeLa cells by subjecting them to a cell viability study using an XTT assay.[32] Following treatment with the compound for 72 h, **12** demonstrated a disappointing IC_{50} > 50 μM (**Fig. 9A**). Additionally, treatment of HEK293T cells, which do not express miR-21, with a serial dilution of compound **12** did not inhibit cell viability, supporting our hypothesis that the compound reduces HeLa cell viability in a miR-21-dependent manner (Fig. S3). To further explore this response and determine if **12**-induced limited cell death was due to triggering of apoptosis, we examined caspase-3/7 activation in HeLa cells. Antisense oligonucleotide-mediated inhibition of miR-21 has been previously shown to inhibit cell proliferation and increase apoptosis of HeLa cells.[33]

ACCEPTED MANUSCRIPT

Treatment of HeLa cells with **12** (10 μM) for 24 h elicited a modest 50% increase in caspase-3/7 activity, a 2-fold increase was observed at an increased concentration of 50 μM (**Fig. 9B**). This suggests that knockdown of miR-21 by **12** leads to a reduction in cell viability by inducing apoptosis, consistent with previous reports.[33-36]

We further explored the therapeutic potential of **12** by investigating the ability of the small molecule to elicit long-term effects in reducing microtumor formation in a clonogenic assay. Oligonucleotide silencing of miR-21 has been shown to inhibit clonogenicity in several cancer cell models[37-39] including cervical cancer.[33,40] Briefly, HeLa cells were suspended in low melt agarose and exposed to a dilution series of **12** for two weeks at 37 ºC prior to imaging (**Fig. S4**). Interestingly, while treatment with **12** only inhibited cell viability at high concentrations, the compound was capable of reducing colony formation of HeLa cells with an EC_{50} of 7.3 μM (**Fig. 9C**). This inhibition of microtumor formation is in good agreement with previous reports that have shown similar results using antisense oligonucleotide-mediated knockdown of miR-21.[33,37,41,42] Furthermore, it was also reported that inhibition or knockout of miR-21 with genetic tools had limited or no effect on cell viability, depending on the cell line,[43,44] while connections between miR-21 and metastasis and tumorigenesis have been observed in a variety of cancers.[45-48]

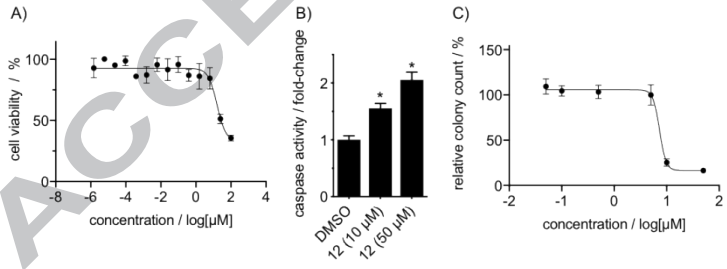

Figure 9. Pre-therapeutic evaluation of **12** in HeLa cells A) Treatment of HeLa cells with **12** for 72 h, followed by a cell viability assay. B) Treatment of HeLa cells with **12** in a two-week clonogenic assay. C) Treatment of HeLa cells with **12** for 24 h, followed by a caspase-3/7 activity assay. Data was normalized to DMSO treatment (negative control) and errors bars represent standard deviations from three independent experiments.

ACCEPTED MANUSCRIPT

3. SUMMARY

In summary, a high-throughput screen for small molecule modulators of miR-21 function led to the identification of a new ether-amide scaffold, and a subsequent structure-activity relationship study of the initial hit compound **1** resulted in the identification of the improved miR-21 inhibitor **12**. Through a biochemical and cell-based firefly luciferase assays as well as a miR-122 reporter cell line, we determined that compound **12** showed selectivity for inhibiting miR-21 function. Furthermore, **12** was found to inhibit transcription of the miR-21 gene resulting in significant reductions in primary and mature miR-21 levels. This mechanism of action is in contrast to other classes of miR-21 inhibitors which appear to inhibit maturation of pre-miR-21[22,25-27] as well as oxadiazole-based inhibitors which appear to inhibit the function of mature miR-21 without affecting miR-21 levels.[24] However, the ether-amide class does appear to follow a similar mechanism to a previously reported azobenzene-based miR-21 inhibitor.[23] Pre-therapeutic evaluation of the lead compound using toxicity and caspase activation assays showed that miR-21 inhibition mediated by **12** reduces cell viability in HeLa cells by inducing apoptosis, although high concentrations are required. However, treatment of HeLa cells with **12** in a long-term clonogenic assay effectively inhibited microtumor formation at low micromolar doses, suggesting that the inhibitor **12** may have potential as a therapeutic for treating miR-21-related diseases.

4. EXPERIMENTAL SECTION

4.1. Chemistry

All reactions were performed in flame-dried glassware under a nitrogen atmosphere and stirred magnetically. Reactions were followed by thin layer chromatography (TLC) using glass-backed silica gel plates (Sorbent Technologies, 250 μm thickness). Anhydrous acetonitrile, tetrahydrofuran (THF) were purchased from Acros and anhydrous toluene, dimethylformamide

ACCEPTED MANUSCRIPT

(DMF) were purchased from Alfa Aesar. Silica gel column chromatography was performed on silica gel (60 Å, 40-63 μm, 230 × 400 mesh, Sorbtech) as a stationary phase. High resolution mass spectral analysis (HRMS) was performed on a Q-Exactive (Thermo Scientific) mass spectrometer. The ^{1}H NMR and ^{13}C NMR spectra were recorded on a 300 MHz or 400 MHz Varian NMR spectrometers. Chemical shifts are given in δ units (ppm) for ^{1}H NMR spectra and ^{13}C NMR spectra.

4.1.1. General procedure for synthesis of compounds **1**, **6**-**18**, **20**-**22**, **24**-**27**, **30**-**40**.

Polyphosphoric acid (10 g) was added to the mixture of 2-aminophenols (or 2-aminothiols or 2-phenylenediamines) **2** (7 - 9 mmol, 1.0 eq) and carboxylic acids **3** (1.0 eq) at room temperature and heated to 170 °C (dissolution of reactants in polyphosphoric acid and effective stirring was observed at elevated temperatures). The reaction mixture was stirred at 170 °C for 3 h and was then allowed to cool to room temperature. The viscous reaction mixture was slowly diluted by ice-water (200 mL), neutralized (to pH 7) by saturated solution of $NaHCO_3$ and extracted with multiple portions of ethyl acetate (3 × 50 mL). The combined organic extracts were washed with brine (50 mL), dried over sodium sulfate (30 g), filtered and concentrated to yield compounds **4** in 24-91% yields as colored solids.

Further, compounds **4** (0.35 - 0.50 mmol, 1.0 eq) were heated with chloroacetyl chloride (3.0 eq) in anhydrous toluene (10 mL) to 90 °C for 2 h. This reaction mixture was concentrated under reduced pressure and the residue was triturated with diethyl ether (10 mL). The product was filtered and subsequently washed with multiple portions of diethyl ether (3 × 5 mL) and dried to recover colored solids. The solids were vigorously stirred in a saturated solution of $NaHCO_3$ (10 mL) for 30 min, acidified to neutral pH by aqueous 1 M HCl solution and then extracted with multiple portions of ethyl acetate (5 × 10 mL) until the aqueous layer turns colorless. The combined organic extracts were washed with brine (10 mL), dried over sodium sulfate (10 g), were filtered and concentrated to yield pure amides **5** as colored solids in 70-90% yield.

ACCEPTED MANUSCRIPT

To a solution of amides **5** (0.08 - 0.44 mmol, 1.0 eq) in anhydrous acetonitrile (5 mL), the indicated phenols, thiophenols, or anilines (1.2 eq) and Cs_2CO_3 (1.2 eq) were added and the reaction mixture was stirred overnight at room temperature. The reaction was quenched by adding water (10 mL) and extracted with ethyl acetate (5 × 10 mL). The combined ethyl acetate extracts were washed with brine (10 mL), dried over sodium sulfate (10 g), filtered and concentrated under reduced pressure. The residual solid was purified by silica gel column chromatography in 1:9 – 7:3 ethyl acetate/hexanes to yield compounds **1**, **6**-**18**, **20**-**22**, **24**-**27**, **30**-**40** in 23% to quantitative yield.

Compounds **6** (PubChem CID 871321) and **7** (PubChem CID 82391) have been previously characterized.

***N*-(4-(Benzo[d]oxazol-2-yl)phenyl)-2-(2-iodophenoxy)acetamide** (**8**). 58 mg, 39% yield; ^{1}H NMR (300 MHz, $CHCl_3$-*d*) δ 9.07 (s, 1H), 8.28 (d, *J* = 8.8 Hz, 1H), 7.89 - 7.76 (m, 4H), 7.61 - 7.58 (m, 1H), 7.40 - 7.32 (m, 2H), 6.88 (t, *J* = 14.4 Hz, 2H), 6.83 - 6.76 (m, 2H), 4.69 (s, 2H). HRMS (ESI) calcd. for $C_{21}H_{15}N_2O_3I$ $(M+H)^+$ 471.0206, found: 471.0226.

***N*-(4-(Benzo[d]oxazol-2-yl)phenyl)-2-phenoxyacetamide** (**9**). 35 mg, 90% yield; ^{1}H NMR (300 MHz, $CHCl_3$-*d*) δ 8.47 (s, 1H), 8.26 (d, J = 8.7 Hz, 2H), 7.82 - 7.75 (m, 3H), 7.61 - 7.55 (m, 1H), 7.40 - 7.33 (m, 3H), 7.08 - 7.00 (dd, *J* = 15.6, 6.6 Hz, 3H), 4.66 (s, 2H). HRMS (ESI) calcd. for $C_{21}H_{16}N_2O_3$ $(M+H)^+$ 345.1239, found: 345.1269.

***N*-(4-(Benzo[d]oxazol-2-yl)phenyl)-2-(4-methoxyphenoxy)acetamide** (**10**). 16 mg, 52% yield; ^{1}H NMR (400 MHz, DMSO-d_6) δ 8.48 (s, 1 H), 8.26 (d, *J* = 8.4 Hz, 2 H), 7.76 - 7.80 (m, 3 H), 7.57 - 7.58 (m, 1 H), 7.34 - 7.36 (m, 2 H), 6.80 - 6.96 (m, 4 H), 4.59 (s, 2 H), 3.79 (s, 3H); HRMS (ESI) calcd. for $C_{22}H_{17}O_4N_2$ $(M+H)^+$ 373.1183, found: 373.1187.

ACCEPTED MANUSCRIPT

***N*-(4-(5-Chlorobenzo[d]oxazol-2-yl)phenyl)-2-phenoxyacetamide** (**11**). 21 mg, 56% yield; ^{1}H NMR (400 MHz, DMSO-d_6) δ 8.47 (s, 1 H), 8.23 (d, *J* = 8.4 Hz, 2 H), 7.80 (d, *J* = 8.8 Hz, 2 H), 7.24 (d, *J* = 2.2 Hz, 1 H), 7.49 (d, *J* = 8.2 Hz, 1 H), 7.37 - 7.39 (m, 2 H), 7.32 - 7.33 (m, 1 H), 7.00 - 7.08, 3 H), 4.65 (s, 2 H); HRMS (ESI) calcd. for $C_{21}H_{16}O_3N_2Cl$ $(M+H)^+$ 379.0844, found: 379.0848.

***N*-(4-(5-Chlorobenzo[d]oxazol-2-yl)phenyl)-2-(4-methoxyphenoxy)acetamide** (**12**). 20 mg, 52% yield; ^{1}H NMR (400 MHz, $CHCl_3$-*d*) δ 8.48 (s, 1 H), 8.23 (d, *J* = 8.2 Hz, 2 H), 7.81 - 7.79 (m, 2 H), 7.72 (d, *J* = 2.2 Hz, 1 H), 7.50 (d, *J* = 8.8 Hz, 2 H), 7.30 - 7.33 (m, 1 H), 6.88 - 6.96 (m, 4 H), 4.60 (s, 2 H), 3.79 (s, 3H); ^{13}C NMR (100 MHz, $CHCl_3$-*d*) δ 166.73, 162.59, 155.14, 151.00, 150.74, 142.16, 139.80, 128.73, 125.03, 124.61, 123.37, 119.90, 119.86, 116.01, 115.02, 110.55, 68.56, 55.73; HRMS (ESI) calcd. for $C_{22}H_{16}O_4N_2Cl$ $(M+H)^+$ 407.0793, found: 407.0796.

***N*-(4-(5-Chloro-1H-benzo[d]imidazol-2-yl)phenyl)-2-(4-methoxyphenoxy)acetamide** (**13**). 22 mg, 58% yield; ^{1}H NMR (400 MHz, DMSO-d_6) δ 13.01 (br s, 1 H), 10.29 (s, 1 H), 8.08 - 8.15 (m, 2 H), 7.80 - 7.87 (m, 2 H), 7.47 - 7.69 (m, 2 H), 7.21 (dd, *J* = 8.4, 1.8 Hz, 1 H), 6.85 - 7.01 (m, 4 H), 4.67 (s, 2 H), 3.70 (s, 3 H); HRMS (ESI) calcd. for $C_{22}H_{19}O_3N_3Cl$ $(M+H)^+$ 408.1109, found: 408.1120.

***N*-(4-(5-Chloro-1H-benzo[d]imidazol-2-yl)phenyl)-2-phenoxyacetamide** (**14**). 21 mg, 60% yield; ^{1}H NMR (400 MHz, DMSO-d_6) δ 13.01 (d, *J* = 12.4 Hz, 1 H), 10.35 (s, 1 H), 8.09 - 8.16 (m, 2 H), 7.80 - 7.87 (m, 2 H), 7.62 - 7.70 (m, 1 H), 7.50 - 7.54 (m, 1 H), 7.30 - 7.36 (m, 2 H), 7.21 (ddd, *J* = 9.9, 8.3, 2.0 Hz, 1 H), 6.96 - 7.04 (m, 3 H), 4.75 (s, 2 H); HRMS (ESI) calcd. for $C_{21}H_{17}O_2N_3Cl$ $(M+H)^+$ 378.1004, found: 378.1007.

***N*-(4-(6-Chlorobenzo[d]oxazol-2-yl)phenyl)-2-phenoxyacetamide** (**16**). 12 mg, 32% yield; ^{1}H NMR (300 MHz, DMSO-d_6) δ 10.41 (s, 1 H), 8.15 (d, *J* = 8.6 Hz, 2 H), 7.89 - 7.99 (m, 3 H), 7.79

ACCEPTED MANUSCRIPT

(d, *J* = 8.5 Hz, 1 H), 7.45 (dd, *J* = 8.4, 2.0 Hz, 1 H), 6.86 - 7.01 (m, 4 H), 4.69 (s, 2 H), 3.70 (s, 3 H); HRMS (ESI) calcd. for $C_{21}H_{16}O_3N_2Cl$ $(M+H)^+$ 379.08440, found: 379.0862.

***N*-(3-(5-Chlorobenzo[d]oxazol-2-yl)phenyl)-2-phenoxyacetamide** (**17**). 23 mg, 62% yield; ^{1}H NMR (300 MHz, DMSO-d_6) δ ppm 8.35 - 8.52 (m, 1 H), 8.31 (s, 1 H), 7.90 - 8.03 (m, 2 H), 7.71 (d, *J* = 1.7 Hz, 1 H), 7.42 - 7.56 (m, 2 H), 7.22 - 7.38 (m, 3 H), 6.96 - 7.09 (m, 2 H), 4.63 (s, 2 H); HRMS (ESI) calcd. for $C_{21}H_{14}O_3N_2Cl$ $(M+H)^+$ 377.0688, found: 377.0697.

***N*-(3-(Benzo[d]oxazol-2-yl)phenyl)-2-phenoxyacetamide** (**18**). 38 mg, 97% yield; ^{1}H NMR (400 MHz, DMSO-d_6) δ 10.41 (s, 1 H), 8.6 (t, *J* = 1.8 Hz, 1 H), 7.9 (dt, *J* = 7.6, 1.3 Hz, 1 H), 7.79 - 7.85 (m, 3 H), 7.67 - 7.79 (m, 1 H), 7.58 (t, *J* = 7.9 Hz, 1 H), 7.41 - 7.47 (m, 2 H), 7.30 - 7.37 (m, 2 H), 6.97 - 7.07 (m, 3 H), 4.76 (s, 2 H); HRMS (ESI) calcd. for $C_{21}H_{17}O_3N_2$ $(M+H)^+$ 345.1233, found: 345.1249.

***N*-(4-(6-Chlorobenzo[d]oxazol-2-yl)phenyl)-2-(4-methoxyphenoxy)acetamide** (**20**). 25 mg, 65% yield; ^{1}H NMR (300 MHz, DMSO-d_6) δ 10.41 (s, 1 H), 8.15 (d, *J* = 8.6 Hz, 2 H), 7.89 - 7.99 (m, 3 H), 7.79 (d, *J* = 8.5 Hz, 1 H), 7.45 (dd, *J* = 8.4, 2.0 Hz, 1 H), 6.86 - 7.01 (m, 4 H), 4.69 (s, 2 H), 3.70 (s, 3 H); HRMS (ESI) calcd. for $C_{22}H_{18}O_4N_2Cl$ $(M+H)^+$ 409.0949, found: 409.0964.

***N*-(3-(5-Chlorobenzo[d]oxazol-2-yl)phenyl)-2-(4-methoxyphenoxy)acetamide** (**21**). 35 mg, 89% yield; ^{1}H NMR (300 MHz, DMSO-d_6) δ 10.36 (s, 1 H), 8.68 (s, 1 H), 7.81 - 7.98 (m, 4 H), 7.45 - 7.62 (m, 2 H), 6.86 - 7.03 (m, 4 H), 4.68 (s, 2 H), 3.70 (s, 3 H); HRMS (ESI) calcd. for $C_{22}H_{18}O_4N_2Cl$ $(M+H)^+$ 409.0949, found: 409.0963.

***N*-(3-(Benzo[d]oxazol-2-yl)phenyl)-2-(4-methoxyphenoxy)acetamide** (**22**). 35 mg, 89% yield; ^{1}H NMR (400 MHz, DMSO-d_6) δ ^{1}H NMR (400 MHz, DMSO-d_6) δ ppm 10.36 (s, 1 H), 8.67 (t, *J* = 1.8 Hz, 1 H), 7.93 (d, *J* = 7.7 Hz, 1 H), 7.85 (br s, 1 H), 7.79 - 7.88 (m, 2 H), 7.58 (t, *J* = 8.0

ACCEPTED MANUSCRIPT

Hz, 1 H), 7.41 - 7.46 (m, 2 H), 6.88 - 7.01 (m, 4 H), 4.69 (s, 2 H); HRMS (ESI) calcd. for $C_{22}H_{19}O_4N_2$ $(M+H)^+$ 375.1339, found: 375.1353.

***N*-(4-(5-Chlorobenzo[d]oxazol-2-yl)phenyl)-2-((4-methoxyphenyl)thio)acetamide** (**24**). 24 mg, 60% yield; ^{1}H NMR (400 MHz, DMSO-d_6) δ ppm 10.49 (s, 1 H), 8.12 - 8.17 (m, 2 H), 7.77 - 7.85 (m, 4 H), 7.39 - 7.47 (m, 3 H), 6.90 - 6.96 (m, 2 H), 3.73 - 3.76 (m, 5 H); HRMS (ESI) calcd. for $C_{22}H_{18}O_3N_2ClS$ $(M-H)^-$ 423.0576, found: 423.0565.

***N*-(4-(5-Chlorobenzo[d]oxazol-2-yl)phenyl)-2-((4-methoxyphenyl)amino)acetamide** (**25**). 11 mg, 29% yield; ^{1}H NMR (300 MHz, DMSO-d_6) δ ppm 10.60 (s, 1 H), 8.16 - 8.22 (m, 3 H), 7.80 - 7.95 (m, 4 H), 7.44 - 7.46 (m, 2 H), 6.89 - 7.06 (m, 2 H), 4.38 (s, 1 H), 4.09 (s, 2 H), 3.70 (s, 3 H); HRMS (ESI) calcd. for $C_{22}H_{19}O_3N_3Cl$ $(M+H)^+$ 408.1109, found: 408.1090.

***N*-(6-(5-Chlorobenzo[d]oxazol-2-yl)naphthalen-2-yl)-2-phenoxyacetamide** (**26**). 32 mg, 87% yield; ^{1}H NMR (300 MHz, DMSO-d_6) δ 10.48 (s, 1 H), 8.76 (s, 1 H), 8.45 (s, 1 H), 8.10 - 8.28 (m, 2 H), 8.04 (d, *J* = 8.7 Hz, 1 H), 7.94 (d, *J* = 2.1 Hz, 1 H), 7.69 - 7.90 (m, 2 H), 7.49 (dd, *J* = 8.6, 2.1 Hz, 1 H), 7.34 (dd, *J* = 8.6, 7.1 Hz, 2 H), 6.93 - 7.10 (m, 3 H), 4.79 (s, 2 H); HRMS (ESI) calcd. for $C_{25}H_{18}O_3N_2Cl$ $(M+H)^+$ 429.1000, found: 429.1012.

***N*-(5-(5-Chlorobenzo[d]oxazol-2-yl)benzo[d]thiazol-2-yl)-2-(4-methoxyphenoxy)acetamide** (**27**). 29 mg, 78% yield; ^{1}H NMR (400 MHz, DMSO-d_6) δ 12.98 (s, 1 H), 8.90 (d, *J* = 1.6 Hz, 1 H), 8.25 (dd, *J* = 8.4, 1.6 Hz, 1 H), 7.91 - 7.96 (m, 3 H), 7.79 - 7.84 (m, 2 H), 7.48 - 7.78 (m, 2H), 6.92 (m, 1 H), 4.51 (s, 2 H); HRMS (ESI) calcd. for $C_{23}H_{17}O_4N_3ClS$ $(M+H)^+$ 466.0623, found: 466.0615.

***N*-(4-(5-Chlorobenzo[d]oxazol-2-yl)phenyl)-2-(3-methoxyphenoxy)acetamide** (**30**). 23 mg, 60% yield; ^{1}H NMR (300 MHz, DMSO-d_6) δ 10.46 (s, 1 H), 8.17 (br d, *J* = 8.4 Hz, 2 H), 7.86 - 7.95 (m, 3 H), 7.81 (d, *J* = 8.6 Hz, 1 H), 7.45 (dd, *J* = 8.6, 2.1 Hz, 1 H), 7.22 (t, *J* = 8.4 Hz, 1 H),

ACCEPTED MANUSCRIPT

6.53 - 6.65 (m, 3 H), 4.75 (s, 2 H), 3.74 (s, 3 H); ^{13}C NMR (75 MHz, DMSO-d_6) δ 167.11, 163.63, 160.44, 158.93, 148.96, 142.94, 142.00, 130.01, 128.94, 128.44, 125.16, 120.79, 119.76, 119.23, 112.11, 106.93, 106.72, 101.15, 67.23, 55.12; HRMS (ESI) calcd. for $C_{20}H_{14}O_3N_2Cl$ $(M+H)^+$ 407.0793, found: 407.0790.

***N*-(4-(5-Chlorobenzo[d]oxazol-2-yl)phenyl)-2-(4-cyanophenoxy)acetamide** (**31**). 21 mg, 53% yield; ^{1}H NMR (300 MHz, DMSO-d_6) δ 10.56 (s, 1 H), 8.17 (d, *J* = 8.7 Hz, 2 H), 7.89 - 7.95 (m, 6 H), 7.44 (dd, *J* = 8.7, 2.1 Hz, 1 H), 7.18 (d, *J* = 8.7 Hz, 2 H), 4.91 (s, 2 H); HRMS (ESI) calcd. for $C_{22}H_{15}O_3N_3Cl$ $(M+H)^+$ 404.0797, found: 404.0803.

***N*-(4-(5-Chlorobenzo[d]oxazol-2-yl)phenyl)-2-(4-fluorophenoxy)acetamide** (**32**). 37 mg, 94% yield; ^{1}H NMR (300 MHz, DMSO-d_6) δ 10.47 (s, 1 H), 8.17 (d, *J* = 8.6 Hz, 2 H), 7.86 - 7.95 (m, 3 H), 7.81 (d, *J* = 8.6 Hz, 1 H), 7.45 (dd, *J* = 8.6, 2.1 Hz, 1 H), 7.11 - 7.20 (m, 2 H), 7.00 - 7.09 (m, 2 H), 4.75 (s, 2 H); HRMS (ESI) calcd. for $C_{21}H_{15}O_3N_2ClF$ $(M+H)^+$ 397.0750, found: 397.0769.

***N*-(4-(5-Chlorobenzo[d]oxazol-2-yl)phenyl)-2-(4-nitrophenoxy)acetamide** (**33**). 10 mg, 23% yield; ^{1}H NMR (300 MHz, DMSO-d_6) δ 10.43 (s, 1 H), 8.13 - 8.20 (m, 3 H), 7.88 - 7.99 (m, 4 H), 7.79 - 7.82 (m, 2 H), 7.25 - 7.49 (m, 2 H), 4.36 (s, 2 H); HRMS (ESI) calcd. for $C_{21}H_{15}O_5N_3Cl$ $(M+H)^+$ 424.0695, found: 424.0674.

2-([1,1'-Biphenyl]-4-yloxy)-N-(4-(5-chlorobenzo[d]oxazol-2-yl)phenyl)acetamide (**34**). 27 mg, 61% yield; ^{1}H NMR (400 MHz, DMSO-d_6) δ ppm 10.54 (s, 1 H), 8.16 - 8.20 (m, 1 H), 7.79 - 8.00 (m, 5 H), 7.61 - 7.66 (m, 1 H), 7.39 - 7.51 (m, 3 H), 7.26 - 7.38 (m, 1 H), 7.11 (d, *J* = 8.8 Hz, 2 H), 4.83 (s, 1 H); HRMS (ESI) calcd. for $C_{27}H_{20}O_3N_2Cl$ $(M+H)^+$ 455.1157, found: 455.1153.

***N*-(4-(5-Chlorobenzo[d]oxazol-2-yl)phenyl)-2-(4-isopropyl-3-methylphenoxy)acetamide** (**35**). 41 mg, 96% yield; ^{1}H NMR (400 MHz, DMSO-d_6) δ ppm 10.45 (s, 1 H), 8.17 (d, *J* = 8.8 Hz, 2 H), 7.79 - 7.98 (m, 4 H), 7.45 (dd, *J* = 8.7, 2.1 Hz, 1 H), 7.16 (d, *J* = 9.3 Hz, 1 H), 6.77 - 6.83

ACCEPTED MANUSCRIPT

(m, 2 H), 4.71 (s, 2 H), 3.03 (sep, *J* = 6.9 Hz, 1 H), 2.27 (s, 3 H), 1.14 (d, *J* = 6.9 Hz, 6 H); HRMS (ESI) calcd. for $C_{25}H_{24}O_3N_2Cl$ $(M+H)^+$ 435.1470, found: 435.1462.

***N*-(4-(5-Fluorobenzo[d]oxazol-2-yl)phenyl)-2-(4-methoxyphenoxy)acetamide** (**36**). 37 mg, 96% yield; ^{1}H NMR (300 MHz, DMSO-d_6) δ 10.43 (s, 1 H), 8.16 (d, *J* = 8.6 Hz, 2 H), 7.91 (d, *J* = 8.6 Hz, 2 H), 7.80 (dd, *J* = 8.9, 4.4 Hz, 1 H), 7.66 (dd, *J* = 8.8, 2.6 Hz, 1 H), 7.27 (td, *J* = 9.3, 2.6 Hz, 1 H), 6.85 - 7.01 (m, 4 H), 4.69 (s, 2 H), 3.70 (s, 3 H); HRMS (ESI) calcd. for $C_{22}H_{18}O_4N_2F$ $(M+H)^+$ 393.1245, found: 393.1264.

***N*-(4-(5-Fluorobenzo[d]oxazol-2-yl)phenyl)-2-phenoxyacetamide** (**37**). 39 mg, quantitative yield; ^{1}H NMR (300 MHz, DMSO-d_6) δ 10.48 (s, 1 H), 8.17 (d, *J* = 8.5 Hz, 2 H), 7.91 (d, *J* = 8.5 Hz, 2 H), 7.80 (dd, *J* = 8.9, 4.4 Hz, 1 H), 7.66 (dd, *J* = 8.8, 2.6 Hz, 1 H), 7.22 - 7.39 (m, 3 H), 6.95 - 7.07 (m, 3 H), 4.76 (s, 2 H); HRMS (ESI) calcd. for $C_{21}H_{16}O_3N_2F$ $(M+H)^+$ 363.1140, found: 363.1149.

***N*-(4-(5-Bromobenzo[d]oxazol-2-yl)phenyl)-2-(4-methoxyphenoxy)acetamide** (**38**). 31 mg, 81% yield; ^{1}H NMR (300 MHz, DMSO-d_6) δ 10.43 (s, 1 H), 8.17 (d, *J* = 8.5 Hz, 2 H), 8.02 (d, *J* = 1.9 Hz, 1 H), 7.91 (d, *J* = 8.6 Hz, 2 H), 7.76 (d, *J* = 8.6 Hz, 1 H), 7.57 (dd, *J* = 8.6, 2.0 Hz, 1 H), 6.86 - 7.00 (m, 4 H), 4.69 (s, 2 H), 3.70 (s, 3 H); ^{13}C NMR (75 MHz, DMSO-d_6) δ 167.44, 163.42, 153.87, 151.74, 149.33, 143.42, 142.04, 128.44, 127.87, 122.14, 120.73, 119.76, 116.68, 115.72, 114.60, 112.60, 67.93, 55.35; HRMS (ESI) calcd. for $C_{22}H_{16}O_4N_2Br$ $(M+H)^+$ 451.0288, found: 451.0307.

2-(4-Methoxyphenoxy)-N-(4-(5-phenylbenzo[d]oxazol-2-yl)phenyl)acetamide (**39**). 28 mg, 70% yield; ^{1}H NMR (300 MHz, DMSO-d_6) δ 10.40 - 10.46 (m, 1 H), 8.20 (br d, *J* = 8.5 Hz, 2 H), 8.03 (d, *J* = 1.7 Hz, 1 H), 7.89 - 7.97 (m, 2 H), 7.84 (d, *J* = 8.6 Hz, 1 H), 7.67 - 7.77 (m, 3 H), 7.46 - 7.54 (m, 2 H), 7.35 - 7.42 (m, 1 H), 6.86 - 7.01 (m, 4 H), 4.69 (s, 2 H), 3.70 (s, 3 H); ^{13}C NMR (75 MHz, DMSO-d_6) δ 167.40, 153.88, 151.76, 149.77, 142.40, 141.76, 140.02, 137.54,

ACCEPTED MANUSCRIPT

128.94, 128.24, 127.34, 127.08, 124.34, 119.79, 117.53, 115.72, 114.61, 110.96, 67.95, 55.35, 40.22; HRMS (ESI) calcd. for $C_{22}H_{16}O_4N_2Cl$ $(M-H)^+$ 407.0793, found: 407.0790.

2-(4-Methoxyphenoxy)-N-(4-(oxazolo[4,5-b]pyridin-2-yl)phenyl)acetamide (**40**). 29 mg, 74% yield; ^{1}H NMR (300 MHz, DMSO-d_6) δ 10.48 (s, 1 H), 8.54 (dd, *J* = 4.8, 1.4 Hz, 1 H), 8.20 - 8.28 (m, 3 H), 7.95 (d, *J* = 8.6 Hz, 2 H), 7.45 (dd, *J* = 8.1, 4.8 Hz, 1 H), 6.87 - 7.02 (m, 4 H), 4.71 (s, 2 H), 3.72 (s, 3 H); HRMS (ESI) calcd. for $C_{21}H_{18}O_4N_3$ $(M+H)^+$ 376.1292, found: 376.1297.

Phenyl (4-(5-chlorobenzo[d]oxazol-2-yl)phenyl)carbamate (**19**). To a solution of 4-(5-chlorobenzo[d]oxazol-2-yl)aniline (50 mg, 1 eq) in anhydrous DCM (5 mL) at 0 °C, phenyl chloroformate (31 µL, 1.2 eq) and triethylamine (42 µL, 1.5 eq) was added. The reaction mixture was warmed to room temperature and stirred for 3 h. The reaction was quenched by water (10 mL) and extracted with multiple portions of ethyl acetate (3 × 5 mL). The combined organic extracts were combined, washed with saturated solution of sodium bicarbonate (10 mL) and brine (10 mL), dried over sodium sulfate (10 g), filtered and concentrated. Compound **19** was purified by silica gel column chromatography in 50% ethyl acetate/hexanes to yield a white solid (62 mg, 83% yield). ^{1}H NMR (400 MHz, DMSO-d_6) δ ppm 10.72 (s, 1 H), 8.15 - 8.20 (m, 2 H), 7.89 (d, *J* = 2.1 Hz, 1 H), 7.81 (d, *J* = 8.6 Hz, 1 H), 7.74 - 7.78 (m, 2 H), 7.42 - 7.48 (m, 3 H), 7.25 - 7.34 (m, 3 H); HRMS (ESI) calcd. for $C_{21}H_{16}ClO_4N_2$ $(M+H)^+$ 365.0688, found: 365.0694.

4-Methoxyphenyl (4-(5-chlorobenzo[d]oxazol-2-yl)phenyl)carbamate (**23**). To a solution of 4-(5-chlorobenzo[d]oxazol-2-yl)aniline (50 mg, 1 eq) in anhydrous DCM (5 mL) at 0 °C, 4-methoxyphenyl chloroformate (36 µL, 1.2 eq) and triethylamine (42 µL, 1.5 eq) was added. The reaction mixture was warmed to room temperature and stirred for 3 h. The reaction was quenched by water (10 mL) and extracted with multiple portions of ethyl acetate (3 × 5 mL). The combined organic extracts were combined, washed with saturated solution of sodium bicarbonate (10 mL) and brine (10 mL), dried over sodium sulfate (10 g), filtered and

ACCEPTED MANUSCRIPT

concentrated. Compound **23** was purified by silica gel column chromatography in 50% ethyl acetate/hexanes to yield a white solid (81 mg, 79% yield). ^{1}H NMR (400 MHz, DMSO-d_6) δ 10.66 (s, 1 H), 8.16 (s, 1 H), 7.89 (d, *J* = 2.1 Hz, 1 H), 7.82 (d, *J* = 8.6 Hz, 1 H), 7.73 - 7.78 (m, 2 H), 7.45 (dd, *J* = 8.6, 2.2 Hz, 1 H), 7.16 - 7.22 (m, 2 H), 6.96 - 7.01 (m, 2 H), 3.78 (s, 3 H); HRMS (ESI) calcd. for $C_{21}H_{16}ClO_4N_2$ $(M+H)^+$ 395.0793, found: 395.0792.

***N*-(4-(5-Chlorobenzo[d]oxazol-2-yl)phenyl)-2-(4-methoxyphenoxy)-N-methylacetamide** (**28**). To a solution of **12** (10 mg, 1.0 eq) in anhydrous THF (1 mL) at 0 °C, LiHMDS (30 µL, 1.2 eq, 1 M in THF) was added the suspension was stirred for 30 min. Methyl iodide (5 µL, 3.3 eq) was added to this solution at 0 °C and the reaction mixture was warmed to room temperature and stirred overnight. Upon complete consumption of **12**, the reaction mixture was concentrated. Compound **28** was purified by silica gel column chromatography in 30% ethyl acetate/hexanes to yield a white solid (8.9 mg, 86% yield). ^{1}H NMR (400 MHz, DMSO-d_6) δ 8.23 (d, *J* = 8.4 Hz, 2 H), 7.94 (d, *J* = 2.0 Hz, 1 H), 7.84 (d, *J* = 8.4 Hz, 1 H), 7.66 (d, *J* = 8.4 Hz, 2 H), 7.48 (dd, *J* = 8.7, 2.4 Hz, 1 H), 6.76 - 6.82 (m, 4 H), 4.63 (br s, 3 H), 3.66 (s, 3 H), 3.30 (s, 3 H); HRMS (ESI) calcd. for $C_{23}H_{20}O_4N_2Cl$ $(M+H)^+$ 423.1106, found: 423.1110.

***N*-(4-(5-Chlorobenzo[d]oxazol-2-yl)phenyl)-2-(4-methoxyphenoxy)-N-(prop-2-yn-1-yl)acetamide** (**29**). To a solution of **12** (50 mg, 1.0 eq) in anhydrous DMF (3 mL) at 0 °C, sodium hydride (6 mg, 60% suspension in mineral oil, 1.2 eq) was added the suspension was stirred for 15 min. Propargyl bromide (22 µL, 1.2 eq, 80 wt% solution in toluene) was added dropwise to this solution at 0 °C and he reaction mixture was warmed to room temperature and stirred overnight. Upon complete consumption of **12**, the reaction mixture was quenched by ice-water mixture (5 mL) and extracted with multiple portions of ethyl acetate (3 × 5 mL). The combined organic extracts were combined, washed with brine (10 mL), dried over sodium sulfate (10 g), filtered and concentrated. Compound **29** was purified by silica gel column chromatography in 30% ethyl acetate/hexanes to yield a yellow solid (24 mg, 44% yield). ^{1}H

ACCEPTED MANUSCRIPT

NMR (300 MHz, DMSO-d_6) δ 8.07 (d, J = 8.9 Hz, 2 H), 7.82 (d, J = 2.1 Hz, 1 H), 7.76 (d, J = 8.7 Hz, 1 H), 7.39 (dd, J = 8.6, 2.2 Hz, 1 H), 7.08 (d, J = 9.1 Hz, 2 H), 6.84 - 6.90 (m, 4 H), 4.31 (d, J = 2.3 Hz, 3 H), 3.57 - 3.65 (m, 1 H), 3.23 (t, J = 2.1 Hz, 2 H); HRMS (ESI) calcd. for $C_{25}H_{20}O_4N_2Cl$ $(M+H)^+$ 447.1106, found: 447.1105.

ASSOCIATED CONTENT

Biological protocols and Supplementary Figures (S1-S3)

Synthetic schemes and analytical data for compounds **12**, **30**, **38**, and **39**.

AUTHOR INFORMATION

Corresponding Author

deiters@pitt.edu

Notes

The authors declare no competing financial interest.

ACKNOWLEDGEMENTS

A.D. acknowledges support by a Research Scholar Grant (120130-RSG-11-066-01-RMC) from the American Cancer Society. Y.N. was supported, in part, by an Andrew Mellon Predoctoral Fellowship. We thank Dr. Bogi Andersen (University of California Irvine) for supplying the miR-21 promoter reporter plasmid.

ACCEPTED MANUSCRIPT

REFERENCES

(1) Duchaine, T. F.; Fabian, M. R. Mechanistic insights into microRNA-mediated gene silencing. *Cold Spring Harb. Perspect. Biol.* **2019,** *11* (3), a032771.

(2) Xu, W.; San Lucas, A.; Wang, Z.; Liu, Y. Identifying microRNA targets in different gene regions. *BMC Bioinformatics.* **2014,** *15 Suppl 7* (Suppl 7), S4-S4.

(3) Cottrell, K. A.; Szczesny, P.; Djuranovic, S. Translation efficiency is a determinant of the magnitude of miRNA-mediated repression. *Sci. Rep.* **2017,** *7* (1), 14884.

(4) Zhang, K.; Zhang, X.; Cai, Z.; Zhou, J.; Cao, R.; Zhao, Y.; Chen, Z.; Wang, D.; Ruan, W.; Zhao, Q.; Liu, G.; Xue, Y.; Qin, Y.; Zhou, B.; Wu, L.; Nilsen, T.; Zhou, Y.; Fu, X.-D. A novel class of microRNA-recognition elements that function only within open reading frames. *Nat. Struct. Mol. Biol.* **2018,** *25* (11), 1019-1027.

(5) Hausser, J.; Syed, A. P.; Bilen, B.; Zavolan, M. Analysis of CDS-located miRNA target sites suggests that they can effectively inhibit translation. *Genome Res.* **2013,** *23* (4), 604-615.

(6) Treiber, T.; Treiber, N.; Meister, G. Regulation of microRNA biogenesis and its crosstalk with other cellular pathways. *Nat. Rev. Mol. Cell Biol.* **2019,** *20* (1), 5-20.

(7) Winter, J.; Jung, S.; Keller, S.; Gregory, R. I.; Diederichs, S. Many roads to maturity: microRNA biogenesis pathways and their regulation. *Nat. Cell Biol.* **2009,** *11* (3), 228.

(8) Yi, R.; Qin, Y.; Macara, I. G.; Cullen, B. R. Exportin-5 mediates the nuclear export of pre-microRNAs and short hairpin RNAs. *Genes Dev.* **2003,** *17* (24), 3011-3016.

(9) Diederichs, S.; Haber, D. A. Dual Role for Argonautes in MicroRNA Processing and Posttranscriptional Regulation of MicroRNA Expression. *Cell* **2007,** *131* (6), 1097-1108.

(10) Rand, T. A.; Petersen, S.; Du, F.; Wang, X. Argonaute2 Cleaves the Anti-Guide Strand of siRNA during RISC Activation. *Cell* **2005,** *123* (4), 621-629.

(11) Hafner, M.; Landthaler, M.; Burger, L.; Khorshid, M.; Hausser, J.; Berninger, P.; Rothballer, A.; Ascano, M., Jr.; Jungkamp, A.-C.; Munschauer, M.; Ulrich, A.; Wardle, G. S.; Dewell, S.; Zavolan, M.; Tuschl, T. Transcriptome-wide identification of RNA-binding protein and microRNA target sites by PAR-CLIP. *Cell* **2010,** *141* (1), 129-141.

(12) Hammond, S. M. An overview of microRNAs. *Adv. Drug Deliv. Rev.* **2015,** *87*, 3-14.

(13) Paul, P.; Chakraborty, A.; Sarkar, D.; Langthasa, M.; Rahman, M.; Bari, M.; Singha, R. K. S.; Malakar, A. K.; Chakraborty, S. Interplay between miRNAs and human diseases. *J. Cell Physiol.* **2018,** *233* (3), 2007-2018.

(14) Piletič, K.; Kunej, T. MicroRNA epigenetic signatures in human disease. *Arch. Toxicol.* **2016,** *90* (10), 2405-2419.

(15) Farooqi, A. A.; Fuentes-Mattei, E.; Fayyaz, S.; Raj, P.; Goblirsch, M.; Poltronieri, P.; Calin, G. A. Interplay between epigenetic abnormalities and deregulated expression of microRNAs in cancer. *Semin. Cancer Biol.* **2019**.

ACCEPTED MANUSCRIPT

(16) Rupaimoole, R.; Slack, F. J. MicroRNA therapeutics: towards a new era for the management of cancer and other diseases. *Nat. Rev. Drug Discov.* **2017,** *16*, 203.
(17) Takahashi, R.-U.; Prieto-Vila, M.; Kohama, I.; Ochiya, T. Development of miRNA-based therapeutic approaches for cancer patients. *Cancer Sci.* **2019,** *110* (4), 1140-1147.
(18) Farazi, T. A.; Hoell, J. I.; Morozov, P.; Tuschl, T. MicroRNAs in human cancer. *Adv. Exp. Med. Biol.* **2013,** *774*, 1-20.
(19) Markou, A.; Zavridou, M.; Lianidou, E. S. miRNA-21 as a novel therapeutic target in lung cancer. *Lung Cancer (Auckland, N.Z.)* **2016,** *7*, 19-27.
(20) Chan, J. K.; Blansit, K.; Kiet, T.; Sherman, A.; Wong, G.; Earle, C.; Bourguignon, L. Y. W. The inhibition of miR-21 promotes apoptosis and chemosensitivity in ovarian cancer. *Gynecol. Oncol.* **2014,** *132* (3), 739-744.
(21) Shen, H.; Zhu, F.; Liu, J.; Xu, T.; Pei, D.; Wang, R.; Qian, Y.; Li, Q.; Wang, L.; Shi, Z.; Zheng, J.; Chen, Q.; Jiang, B.; Shu, Y. Alteration in Mir-21/PTEN expression modulates gefitinib resistance in non-small cell lung cancer. *PloS One* **2014,** *9* (7), e103305-e103305.
(22) Naro, Y.; Thomas, M.; Stephens, M. D.; Connelly, C. M.; Deiters, A. Aryl amide small-molecule inhibitors of microRNA miR-21 function. *Bioorg. Med. Chem. Lett.* **2015,** *25* (21), 4793-4796.
(23) Gumireddy, K.; Young, D. D.; Xiong, X.; Hogenesch, J. B.; Huang, Q.; Deiters, A. Small-molecule inhibitors of microrna miR-21 function. *Angew. Chem. Int. Ed. Engl.* **2008,** *47* (39), 7482-7484.
(24) Naro, Y.; Ankenbruck, N.; Thomas, M.; Tivon, Y.; Connelly, C. M.; Gardner, L.; Deiters, A. Small Molecule Inhibition of MicroRNA miR-21 Rescues Chemosensitivity of Renal-Cell Carcinoma to Topotecan. *J. Med. Chem.* **2018,** *61* (14), 5900-5909.
(25) Connelly, C. M.; Boer, R. E.; Moon, M. H.; Gareiss, P.; Schneekloth, J. S. Discovery of Inhibitors of MicroRNA-21 Processing Using Small Molecule Microarrays. *ACS Chem. Biol.* **2017,** *12* (2), 435-443.
(26) Velagapudi, S. P.; Costales, M. G.; Vummidi, B. R.; Nakai, Y.; Angelbello, A. J.; Tran, T.; Haniff, H. S.; Matsumoto, Y.; Wang, Z. F.; Chatterjee, A. K.; Childs-Disney, J. L.; Disney, M. D. Approved Anti-cancer Drugs Target Oncogenic Non-coding RNAs. *Cell Chem. Biol.* **2018,** *25* (9), 1086-1094.e7.
(27) Bose, D.; Jayaraj, G.; Suryawanshi, H.; Agarwala, P.; Pore, S. K.; Banerjee, R.; Maiti, S. The Tuberculosis Drug Streptomycin as a Potential Cancer Therapeutic: Inhibition of miR-21 Function by Directly Targeting Its Precursor. *Angew. Chem. Int. Ed. Engl.* **2012,** *51* (4), 1019-1023.
(28) Shi, Z.; Zhang, J.; Qian, X.; Han, L.; Zhang, K.; Chen, L.; Liu, J.; Ren, Y.; Yang, M.; Zhang, A.; Pu, P.; Kang, C. AC1MMYR2, an Inhibitor of Dicer-Mediated Biogenesis of Oncomir miR-21, Reverses Epithelial–Mesenchymal Transition and Suppresses Tumor Growth and Progression. *Cancer Res.* **2013,** *73* (17), 5519-5531.
(29) Thorne, N.; Shen, M.; Lea, Wendy A.; Simeonov, A.; Lovell, S.; Auld, Douglas S.; Inglese, J. Firefly Luciferase in Chemical Biology: A Compendium of Inhibitors,

ACCEPTED MANUSCRIPT

Mechanistic Evaluation of Chemotypes, and Suggested Use As a Reporter. *Chem. Biol.* **2012,** *19* (8), 1060-1072.

(30) Thorne, N.; Inglese, J.; Auld, D. S. Illuminating insights into firefly luciferase and other bioluminescent reporters used in chemical biology. *Chem. Biol.* **2010,** *17* (6), 646-657.

(31) Young, D. D.; Connelly, C. M.; Grohmann, C.; Deiters, A. Small Molecule Modifiers of MicroRNA miR-122 Function for the Treatment of Hepatitis C Virus Infection and Hepatocellular Carcinoma. *J. Am. Chem. Soc.* **2010,** *132* (23), 7976-7981.

(32) Scudiero, D. A.; Shoemaker, R. H.; Paull, K. D.; Monks, A.; Tierney, S.; Nofziger, T. H.; Currens, M. J.; Seniff, D.; Boyd, M. R. Evaluation of a Soluble Tetrazolium/Formazan Assay for Cell Growth and Drug Sensitivity in Culture Using Human and Other Tumor Cell Lines. *Cancer Res.* **1988,** *48* (17), 4827-4833.

(33) Du, G.; Cao, D.; Meng, L. miR-21 inhibitor suppresses cell proliferation and colony formation through regulating the PTEN/AKT pathway and improves paclitaxel sensitivity in cervical cancer cells. *Mol. Med. Rep.* **2017,** *15* (5), 2713-2719.

(34) Gu, J.-B.; Bao, X.-B.; Ma, Z. Effects of miR-21 on proliferation and apoptosis in human gastric adenocarcinoma cells. *Oncol. Lett.* **2018,** *15* (1), 618-622.

(35) Zhou, B.; Wang, D.; Sun, G.; Mei, F.; Cui, Y.; Xu, H. Effect of miR-21 on Apoptosis in Lung Cancer Cell Through Inhibiting the PI3K/ Akt/NF-κB Signaling Pathway *Cellular Physiol. Biochem*. **2018,** *46* (3), 999-1008.

(36) Najafi, Z.; Sharifi, M.; Javadi, G. Degradation of miR-21 induces apoptosis and inhibits cell proliferation in human hepatocellular carcinoma. *Cancer Gene Ther.* **2015,** *22* (11), 530.

(37) Wagenaar, T. R.; Zabludoff, S.; Ahn, S.-M.; Allerson, C.; Arlt, H.; Baffa, R.; Cao, H.; Davis, S.; Garcia-Echeverria, C.; Gaur, R.; Huang, S.-M. A.; Jiang, L.; Kim, D.; Metz-Weidmann, C.; Pavlicek, A.; Pollard, J.; Reeves, J.; Rocnik, J. L.; Scheidler, S.; Shi, C.; Sun, F.; Tolstykh, T.; Weber, W.; Winter, C.; Yu, E.; Yu, Q.; Zheng, G.; Wiederschain, D. Anti–miR-21 Suppresses Hepatocellular Carcinoma Growth via Broad Transcriptional Network Deregulation. *Mol. Cancer Res.* **2015,** *13* (6), 1009-1021.

(38) Lam, H. C.; Liu, H.-J.; Baglini, C. V.; Filippakis, H.; Alesi, N.; Nijmeh, J.; Du, H.; Lope, A. L.; Cottrill, K. A.; Handen, A. Rapamycin-induced miR-21 promotes mitochondrial homeostasis and adaptation in mTORC1 activated cells. *Oncotarget* **2017,** *8* (39), 64714.

(39) Wang, P.; Guan, Q.; Zhou, D.; Yu, Z.; Song, Y.; Qiu, W. miR-21 Inhibitors Modulate Biological Functions of Gastric Cancer Cells via PTEN/PI3K/mTOR Pathway. *DNA Cell Biol.* **2018,** *37* (1), 38-45.

(40) Yao, Q.; Xu, H.; Zhang, Q.-Q.; Zhou, H.; Qu, L.-H. MicroRNA-21 promotes cell proliferation and down-regulates the expression of programmed cell death 4 (PDCD4) in HeLa cervical carcinoma cells. *Biochem. Biophys. Res. Commun.* **2009,** *388* (3), 539-542.

ACCEPTED MANUSCRIPT

(41) Zhang, H.-L.; Si, L.-B.; Zeng, A.; Long, F.; Qi, Z.; Zhao, R.; Bai, M. MicroRNA-21 antisense oligonucleotide improves the sensitivity of A375 human melanoma cell to Cisplatin: An in vitro study. *J. Cell Biochem.* **2018,** *119* (4), 3129-3141.
(42) Misawa, A.; Katayama, R.; Koike, S.; Tomida, A.; Watanabe, T.; Fujita, N. AP-1-Dependent miR-21 expression contributes to chemoresistance in cancer stem cell-like SP cells. *Oncol. Res.* **2010,** *19* (1), 23-33.
(43) Chen, B.; Chen, X.; Wu, X.; Wang, X.; Wang, Y.; Lin, T.-Y.; Kurata, J.; Wu, J.; Vonderfecht, S.; Sun, G.; Huang, H.; Yee, J.-K.; Hu, J.; Lin, R.-J. Disruption of microRNA-21 by TALEN leads to diminished cell transformation and increased expression of cell-environment interaction genes. *Cancer Lett.* **2015,** *356* (2 Pt B), 506-516.
(44) Xiong, G.; Huang, Z.; Jiang, H.; Pan, Z.; Xie, J.; Wang, S. Inhibition of microRNA-21 decreases the invasiveness of fibroblast-like synoviocytes in rheumatoid arthritis via TGFβ/Smads signaling pathway. *Iran. J. Basic Med. Sci.* **2016,** *19* (7), 787-793.
(45) Medina, P. P.; Nolde, M.; Slack, F. J. OncomiR addiction in an in vivo model of microRNA-21-induced pre-B-cell lymphoma. *Nature* **2010,** *467*, 86.
(46) Yang, C. H.; Yue, J.; Pfeffer, S. R.; Handorf, C. R.; Pfeffer, L. M. MicroRNA miR-21 Regulates the Metastatic Behavior of B16 Melanoma Cells. *j. Biol. Chem.* **2011,** *286* (45), 39172-39178.
(47) Nedaeinia, R.; Sharifi, M.; Avan, A.; Kazemi, M.; Nabinejad, A.; Ferns, G. A.; Ghayour-Mobarhan, M.; Salehi, R. Inhibition of microRNA-21 via locked nucleic acid-anti-miR suppressed metastatic features of colorectal cancer cells through modulation of programmed cell death 4. *Tumor Biol.* **2017,** *39* (3), 1010428317692261.
(48) Liu, Z.-L.; Wang, H.; Liu, J.; Wang, Z.-X. MicroRNA-21 (miR-21) expression promotes growth, metastasis, and chemo- or radioresistance in non-small cell lung cancer cells by targeting PTEN. *Mol. Cell Biochem.* **2013,** *372* (1), 35-45.

ACCEPTED MANUSCRIPT

ACCEPTED MANUSCRIPT

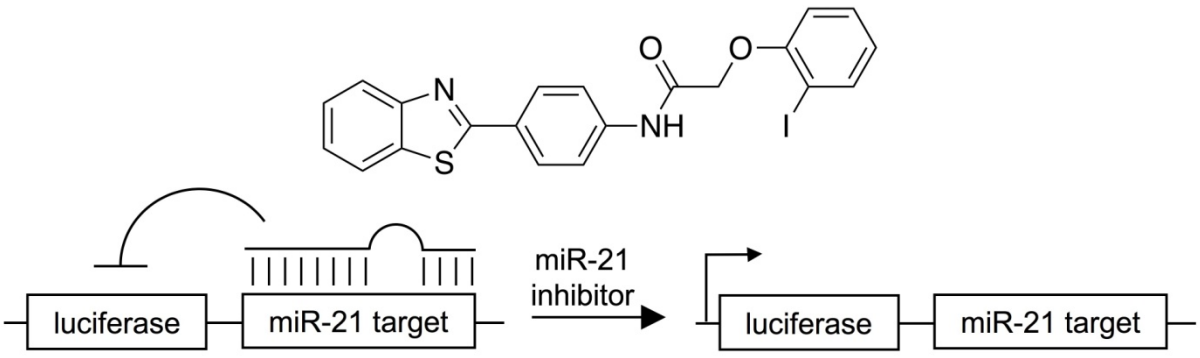

ACCEPTED MANUSCRIPT